Determination of DNA-Base Orientation on Carbon Nanotubes through Directional Optical Absorbance

Sheng Meng,[†] Wei L. Wang,[†] Paul Maragakis,[‡] and Efthimios Kaxiras*,[†]

Department of Physics and School of Engineering and Applied Sciences, Harvard University, Cambridge, Massachusetts 02138, and D. E. Shaw Research, New York, New York, 10036

ABSTRACT

We develop an approach for determining the orientation of DNA bases attached to carbon nanotubes (CNTs), by combining ab initio time-dependent density functional theory and optical spectroscopy measurements. The structures we find are in good agreement with the geometry of nucleosides on a (10,0) CNT obtained from molecular simulations using empirical force fields. The results shed light into the complex interactions of the DNA−CNT system, a candidate for ultrafast DNA sequencing through electronic probes.

The interaction between DNA and carbon nanotubes (CNTs) is a subject of intense current interest. Single-strand DNA (ssDNA) of different lengths, either small oligomers consisting of tens of bases[1,2] or long genomic strands (≫100 bases),[3] have been found to wrap around single-walled CNTs forming tight helices. ssDNA and CNTs have complementary structural features which make it possible to assemble them into a single, stable structure: ssDNA is a flexible, amphiphilic biopolymer while CNTs are stiff, strongly hydrophobic nanorods. A variety of applications for the DNA−CNT system are being explored, such as DNA transporters,[4,5] biosensors,[6] field effect transistors,[7] and agents for CNT dispersion and sorting in solution.[2,1] There is also an increasing interest in the use of CNTs for supporting and detecting DNA through electronic[8] and optical means,[9,10] which could lead to ground-breaking, ultrafast DNA sequencing. Electronic detection of DNA bases using transverse conductance measurements depends sensitively on the tip−base distance and relative orientation, factors that can overwhelm the signal dependence on base identity and severely limit the efficacy of single-base detection methods.[11,12] These difficulties may be overcome in the combined DNA−CNT system, since, as we show in this work, attaching DNA on a CNT fixes the base geometry on the CNT wall.

While the idea of using CNT as a template to hold and fix the DNA bases for electronic detection appears promising, many issues remain to be resolved before it is proven useful. The fundamental aspects of the DNA−CNT interaction at the atomic level, including binding geometries and base orientation, and their dependence on the base identity, remain elusive. The DNA−CNT combined system is a complicated, dynamic structure, in which the four types of bases interact with the CNT in the presence of thermal fluctuations. Individual DNA bases can be stabilized on CNTs through mainly weak van der Waals interaction to the graphitic CNT wall. This interaction is perturbed by the sugar and phosphate groups in the DNA backbone, the counterions that bind to ssDNA, and the water molecules from solution. The first step in attempting to understand this system is to establish whether or not a preferred orientation for each type of base exists.

To address this problem, we investigate the interaction of DNA bases with single-wall CNTs by combining ab initio calculations based on time-dependent density functional theory (TDDFT) and available optical spectroscopic measurements. The optical absorbance spectrum, especially when using a polarized light source, is a signature of the electronic structure of the interacting system, which in turn depends on the precise spacial organization of its components. The intrinsic absorbance of CNTs, for radiation in the UV range of wavelengths 210−260 nm, is highly anisotropic, mainly in the direction perpendicular to the tube axis.[13] Thus, only the component of the electric field along the nanotube axis is relevant. By comparing the calculated orientation-dependent optical absorbance of DNA bases to experimental data, we can determine the orientation of DNA bases relative to the nanotube axis. The resulting orientations agree with the geometry of the bases from empirical force-field simulations of single nucleosides on a (10,0) CNT (a variety that is

---

† Harvard University.
‡ D. E. Shaw Research.

abundant in nanotube samples). This confirmation of atomistic scale structure provided by the different approaches, which encompass theoretical and experimental information, elucidates the geometric features of the DNA−CNT system that are at the core of ultrafast DNA sequencing through electronic means.

Optical absorbance of a molecule along a certain light-polarization direction can be obtained from TDDFT within linear response regime, by applying a finite electric field along that direction which involves transition dipoles projected on that direction only. In practice, this is achieved by applying an electric field along three orthogonal axes separately and then performing a rotation operation to align one axis to the target orientation. Our TDDFT calculations were carried out with the siesta package,[14] using Troullier−Martins pseudopotentials to represent the atomic cores, the Ceperley−Alder local density approximation to the exchange-correlation functional, and a basis of double-ζ polarized atomic orbitals including 13 orbitals for C, N, and O and 5 orbitals for H atoms (more details are given in ref 15). We used 12 212 steps in time to propagate the wavefunctions, with a time step of 3.4×10^{-3} fs, which gives an energy resolution of 0.05 eV and a perturbing external electric field of 0.1 V/Å. A Gaussian smearing width of 0.1 eV is used when plotting the spectra.

The geometry of nucleosides on the (10,0) CNT was determined with the charmm package.[16] We augmented the available force fields for nucleosides[17] with an interaction for the CNT[18] and performed an extensive search of the potential energy surface of each adsorbed nucleoside with the successive confinement method.[19] As the dominant force stabilizing DNA bases on CNT is of the van der Waals type, we expect the DNA−CNT interaction to be less dependent on the electronic properties of the nanotube (metallic or semiconducting) than on its structural parameters such as diameter and chirality.

We analyze first the optical properties of isolated DNA bases, which will set the stage for understanding their spectra when in contact with the CNT. Figure 1 shows our calculated directional optical absorbance spectra and corresponding linear dichroism (LD) spectra of adenine (**A**). The orientation of **A** is defined by the angle of the incident light polarization with respect to the short axis of the molecule, shown in the inset of Figure 1, as per the Devoe−Tinoco convention.[20] The calculated absorbance spectra of **A** show strong dependence on the molecular orientation. There are five absorption peaks in the wavelength range $\lambda > 200$ nm at 284, 257, 227, 217, and 203 nm, identified in Figure 1a, in excellent agreement with experiments, measured at 272, 258, 230, 214, and 207 nm in stretched polymer films[21] and at 274, 254, 213, and 202 nm in crystals.[22] Their intensity varies significantly as a function of the orientation angle from $\theta = -90°$ to $\theta = 90°$. For example, the 284 nm peak has its largest intensity at $\theta \sim 60°$, while it diminishes to almost zero at $\theta \sim -30°$; other peaks exhibit similar behavior. This leads to what may appear as shifts of the peaks in the absorption spectrum: the peak at 284 nm shifts to 257 nm when θ changes from $-90°$ to $-30°$ while the peak at 217
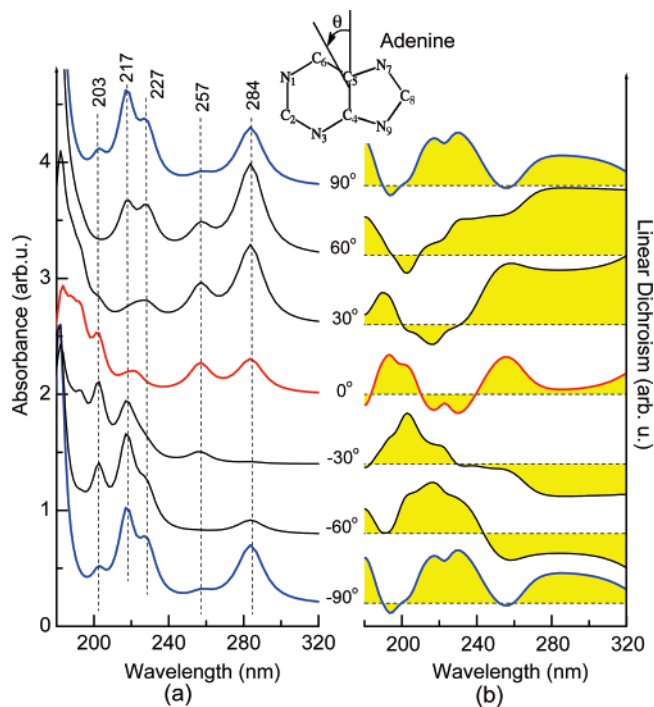

Figure 1. (a) Directional absorption spectra and (b) linear dichroism of adenine, plotted at angles every 30° ranging from −90° to 90° (defined relative to the short molecular axis in the inset). The horizontal lines in (b) indicate zero values.

nm shifts to 227 nm when θ changes from $-30°$ to $30°$. This behavior complicates the interpretation of experiments due to preferred absorption along certain directions.

The strong orientation-dependent absorbance of **A** leads to clear and easily resolved signals in the linear dichroism spectrum, which by definition captures anisotropic absorbance[23]

$$\text{LD} = \frac{I_{\parallel} - I_{\perp}}{I} = \frac{3}{2}(3 \cos^2 \theta_t - 1)$$

Here $I_{\parallel}$ and $I_{\perp}$ represent absorption of light polarized in directions parallel and perpendicular to the direction of orientation, and I is the normal isotropic absorption averaged over all possible orientations. θ_t is the angle between transition moments and the orientation axis. The experimentally measured LD contains an additional multiplicative prefactor S that reflects the order of orientation ($S = 0$ for isotropic samples and $S = 1$ for perfect orientation). The calculated LD spectra of **A** for orientation angles ranging from $\theta = -90°$ to $90°$ is shown in Figure 1b. This signal shows positive or negative peaks at the wavelength of absorbed photons, depending on the orientation. The drastic changes in the spectrum, especially the change in sign at certain wavelengths, is a very sensitive measure of relative orientation of the base and the polarization direction of light. We have discussed **A** in some detail, but similar comments apply to the other three bases; agreement with experiment is typically very satisfactory, especially for the first few lowest energy (longest wavelength) excitations (accuracy within ±0.2 eV).

We next examine the calculated orientation-dependent absorption spectra of DNA bases in the context of bases adsorbed on single-wall CNTs. To this end, we compare the spectrum of the DNA base along each direction with the experimentally measured one for the combined ssDNA–CNT systems. Hughes et al.[24] have recently measured the UV–vis absorption of a DNA homopolymer consisting of ~30 bases wrapped around a CNT. The difference between absorption by the DNA–CNT combined system and the isolated, bare CNT constitutes the absorption signature of the DNA strand attached to the CNT wall. In these experimental measurements, there are significant changes in the spectrum of DNA on the CNT compared with that of free ssDNA in solution, which are characteristic for the four DNA bases. For instance, the first peak centered at 260 nm for free poly(d**A**) is red-shifted to 266 nm when **A** is adsorbed on CNT, and the peak at 203 nm is shifted to 213 nm. Similar changes are found in the difference spectra of the other three bases. For cytosine (**C**), the broad peak at 230–250 nm diminishes, the peak at 200 nm is reduced by half, while the peak at the longest wavelength (310 nm) does not change. For guanine (**G**), the peak at 275 nm remains constant while the peak at 248 nm is reduced by half and the peak at 200 nm increases slightly after adsorption on CNT. For thymine (**T**), there is no apparent change for the peak at 270 nm, while the adsorption in the range of 210–240 nm is significantly reduced. We found that all these features can be reproduced accurately in our calculations by considering the absorption of the base along a certain direction only. In doing this, we search for the field vector orientation θ that minimizes the error function

$$\sigma(\theta) \equiv \int [\delta f(\lambda - \lambda_0, \theta) - \delta f^{\,0}(\lambda)]^2 \, d\lambda$$

here δf is the difference between the absorbance along θ and the isotropic absorbance (averaged over all directions) of the base and $\delta f^{\,0}$ is the experimental spectrum difference due to DNA adsorption on the CNT. λ is the wavelength, and λ_0 accounts for the peak position shift due to errors of calculated excitation energies in TDDFT. Therefore the resulted θ is the field direction that best reproduces the effects seen in experiment. The corresponding absorption is shown in Figure 2, along with the isotropic absorption of the free base for comparison; the direction which produces optimal agreement with experiment is also indicated in each case. A quantitative comparison between experimental and theoretical data is available in Supporting Information. It is a well-established fact that the sugar and the phosphate groups do not make significant contributions to the DNA optical absorption in the UV region $\lambda > 200$ nm,[25] so we ignore these contributions.

The agreement with experiment strongly suggests that there is a preferred absorption direction for the bases on the CNT. The intrinsic absorption of carbon nanotubes is dominant in the UV region $200 < \lambda < 300$ nm, where there are two intrinsic, diameter-independent peaks at 276 and 236 nm, corresponding to directions parallel and perpendicular to the nanotube axis, respectively, with the latter having
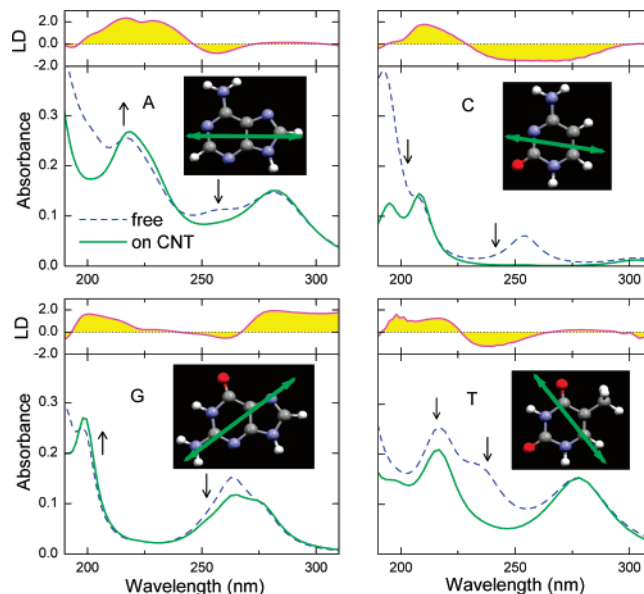

Figure 2. Absorption spectrum of DNA bases averaged over all field directions (dashed line) and along a particular direction (solid line) indicated by arrows which mimics the nanotube axis. These spectra reproduce adequately the experimentally measured spectra in solutions. A larger smearing width than in Figure 1 is used for better comparison. Vertical arrows indicate intensity changes ("↑" for increase and "↓" for decrease) in experimental spectra after base adsorption on the CNT (ref 24). Linear dichroism spectra that best match experiment (ref 23) are also shown at the top of each panel.

larger intensity.[13] Therefore, in the range of interest, 200–260 nm, where the main changes in the absorption spectrum are found for the combined DNA–CNT system, CNT absorption in the perpendicular direction is much larger than absorption in the parallel direction. Consequently, there are more photons with polarization parallel to the CNT axis left available to interact with attached DNA bases or, equivalently, the nanotube produces a local electric field aligned along its axis. The polarizability might be screened by the bound DNA strand, depending on its density and geometry, and in turn on the nanotube diameter and chirality. Thermal fluctuations of counterions and water will average out to a zero contribution to the local field around the DNA–CNT system. This would result in more absorption by the base in the direction parallel to the tube axis than perpendicular to it (this effect is called "hypochroism"). This explains why the absorption spectra of the DNA bases change when they are attached to the nanotube wall—the direction of tube axis is indeed the preferred direction for UV absorption by the bases. Therefore, the arrows in Figure 2 showing the field direction that gives closest agreement with experiment, must be aligned with the nanotube axis. This provides a way to determine the base orientation relative to the nanotube axis in the DNA–CNT system from the optical absorption data. Other possible factors such as different protonation states of DNA bases were also considered; we find that the effects they produce are not consistent with the experimentally observed changes in optical spectra upon DNA adsorption on CNT.

This result is further supported by the comparison between the calculated LD curves and the measured ones. Rajendra
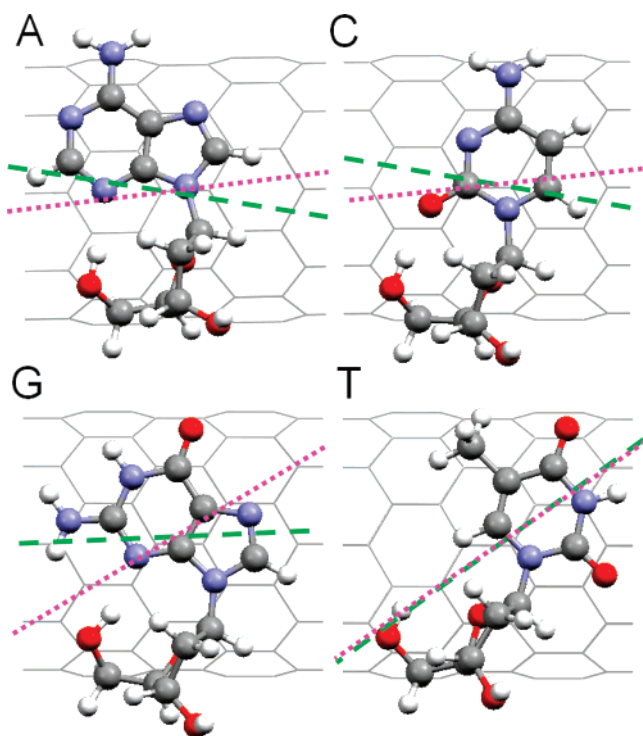
Figure 3. Calculated geometries of DNA nucleosides on CNT (10,0). Lines indicate the orientation of the nanotube axis derived from experimental data: the dashed line is obtained from ultraviolet absorbance spectroscopy; the dotted line from linear dichroism.

and Rodger have measured the LD spectra for the ssDNA with a random sequence and of poly(d**A**) wrapped on a CNT.[23] They observed interesting features: LD spectra for all DNA bases attached to CNT (obtained by subtracting the contribution of CNT from the spectrum of the combined system) show a positive peak at ∼225 nm and a negative peak at ∼275 nm (260 nm for poly(d**A**)). This observation cannot be explained by hypochriosm *solely* because: (i) adsorption of peptide nucleic acid (PNA) on CNT, which should have the same hypochriosm effect if any, shows a negative signal at ∼230 nm and a positive one at ∼270 nm, opposite to what would happen due to hypochriosm; (ii) the peak position depends on the base identity, indicating that this is an intrinsic property of the bases. Therefore the observed behavior implies that the bases on the CNT must have a preferred orientation. Indeed, the best-fit LD spectra show exactly the same behavior as observed in experiment, namely, a positive peak at 220−230 nm and a negative peak at 260−270 nm, as shown in the upper panels of Figure 2.

Figure 3 shows the base orientations with respect to the nanotube axis, along which the experimental absorbance and LD data for DNA wrapped on CNTs are best reproduced. The directions indicated by dashed lines are from absorbance measurements and those by dotted lines are from LD measurements, respectively. These directions correspond to the averaged directions of the nanotube axis in the experimental setup, determined from the measured optical data. There is a surprisingly good agreement between the orientation of the nanotube axis determined this way and that from structure optimization using force field methods. We have performed an extensive search of the potential energy surface

of each adsorbed nucleoside on the CNT (10,0). The search returned ∼1000 distinct potential energy minima for each nucleoside/CNT system. The room-temperature populations of each minimum range from 10^{-10} to ∼50%. As we did not include the influence of base−base interaction in our structural search−these resulting configurations should be considered as averaged conformation. In Figure 3, only the most stable configuration, which has a population weight of 46% for **G**, 28% for **A**, 25% for **C**, and 7% for **T**, is shown for each base. The corresponding interaction energy between each nucleoside and the CNT is 0.81 eV for **A**, 0.85 eV for **G**, 0.70 eV for **C**, and 0.77 eV for **T**; different orientations result in interaction energy differences around 0.1 eV. In Figure 3 the orientation of the nanotube axis relative to the bases agrees well with the tube axis directions determined above, except perhaps for **T**. Specifically, the directions of the nanotube axis from absorbance spectra, linear dichroism, and structural optimization are 89°, 105°, 98° for **A**, −100°, −84°, −90° for **C**, −58°, −30°, −61° for **G**, and 39°, 40°, 75° for **T**. Overall the agreement between experiment and theory is excellent. The difference between angles determined by different approaches is generally within the accuracy of the current method ∼5−10°. Our geometries are not identical to those offered in refs 23 and 24 as possibilities to account for their experimental observations. Note that those possible structures are not obtained by any kind of quantitative analysis but aligning one of the transition moments to the nanotube axis. Moreover, in reality it is possible there exists a mixture of binding configurations for each base; here we focus only on the dominant one. The largest discrepancy occurs in the case of **T**, of order ∼35° between the two extreme positions. This is not surprising considering the small weight of the particular **T** orientation on the CNT from the structural optimization. In our simulations, **T** is the most mobile nucleoside on CNT and thus there are several energetically comparable structures for **T** on the CNT. Indeed, averaging the first few configurations with the largest population improves significantly the agreement between theory and experiment.

In conclusion, we find that the bases in the ssDNA/CNT structure prefer to have a definite orientation relative to the nanotube axis, a feature favoring ultrafast DNA sequencing based on this system. The orientation depends on the base identity and is less sensitive to the diameter and chirality of the CNT, as determined from comparisons between theoretical and experimental optical spectroscopy. The unique orientations of the DNA bases on CNT might originate from the van der Waals interaction between the bases and the curved CNT walls, which would tend to maximize the base−CNT contact region. The sugar and phosphate groups in the DNA backbone might also contribute to this interaction providing further geometrical constrains.

Supporting Information Available: Comparison of experimental (ref 24) and theoretical difference in absorption spectra before and after DNA bases binding on the CNT. This material is available free of charge via the Internet at http://pubs.acs.org.

References

(1) Zheng, M.; Jagota, A.; Semke, E. D.; Diner, B. A.; Mclean, R. S; Lustig, S. R.; Richardson, R. E.; Tassi, N. G. *Nat. Mater.* **2003**, *2*, 338.

(2) Zheng, M.; Jagota, A.; Strano, M. S.; Santos, A. P.; Barone, P.; Chou, S. G.; Diner, B. A.; Dresselhaus, M. S.; Mclean, R. S.; Onoa, G. B.; Samsonidze, G. G.; Semke, E. D.; Usrey, M.; Walls, D. J. *Science* **2003**, *302*, 1545.

(3) Gigliotti, B.; Sakizzie, B.; Bethune, D. S.; Shelby, R. M.; Cha, J. N. *Nano Lett.* **2006**, *6*, 159.

(4) Gao, H.; Kong, Y. *Annu. Rev. Mater. Res.* **2004**, *34*, 123.

(5) Kam, N. W. S.; Liu, Z.; Dai, H. *Angew. Chem., Int. Ed.* **2005**, *45*, 577.

(6) Staii, C.; Johnson, A. T.; Chen, M.; Gelperin, A. *Nano Lett.* **2005**, *5*, 1774.

(7) Lu, Y.; Bangsaruntip, S.; Wang, X.; Zhang, L.; Nishi, Y.; Dai, H. *J. Am. Chem. Soc.* **2006**, *128*, 3518.

(8) Star, A.; Tu, E.; Niemann, J.; Gabriel, J. P.; Joiner, C. S.; Valcke, C. *Prod. Natl. Acad. Sci. of U.S.A.* **2006**, *103*, 921.

(9) Jeng, E. S.; Moll, A. E.; Roy, A. C.; Gastala, J. B.; Strano, M. S. *Nano Lett.* **2006**, *6*, 371.

(10) Heller, D. A.; Jeng, E. S.; Yeung, T. K.; Martinez, B. M.; Moll, A. E.; Gastala, J. B.; Strano, M. S. *Science* **2006**, *311*, 508.

(11) Zhan, X. G.; Krstic, P. S.; Zikic, R.; Wells, J. C.; Fuentes-Cabrera, M. *Biophys. J.* **2006**, *91*, L04.

(12) Zwolak, M.; Di Ventra, M. *Nano Lett.* **2005**, *5*, 421.

(13) Murakami, Y.; Einarsson, E.; Edamura, T.; Maruyama, S. *Phys. Rev. Lett.* **2005**, *94*, 087402.

(14) Sanchez-Portal, D.; Ordejon, P.; Artacho, E.; Soler, J. M. *Int. J. Quantum Chem.* **1997**, *65*, 453.

(15) Tsolakidis, A.; Kaxiras, E. *J. Phys. Chem. A* **2005**, *109*, 2373.

(16) Brooks, B. R.; Bruccoleri, R. E.; Olafson, B. D.; States, D. J.; Swaminathan, S.; Karplus, M. *J. Comput. Chem.* **1983**, *4*, 187.

(17) MacKerell, A. D., Jr.; Bashford, D.; Bellott, R. L.; Dunbrack, R. L., Jr.; Evanseck, J. D.; Field, M. J.; Fischer, S.; Gao, J.; Guo, H.; Ha, S.; Joseph-McCarthy, D.; Kuchnir, L.; Kuczera, K.; Lau, F. T. K.; Mattos, C.; Michnick, S.; Ngo, T.; Nguyen, D. T.; Prodhom, B.; Reiher, W. E., III; Roux, B.; Schlenkrich, M.; Smith, J. C.; Stote, R.; Straub, J.; Watanabe, M.; Wiorkiewicz-Kuczera, J.; Yin, D.; Karplus, M. J. *J. Phys. Chem. B* **1998**, *102*, 3586.

(18) Lu, G.; Maragakis, P.; Kaxiras, E. *Nano Lett.* **2005**, *5*, 897.

(19) Krivov, S. V.; Chekmarev, S. F.; Karplus, M. *Phys. Rev. Lett.* **2002**, *88*, 038101.

(20) Broo, A.; Holmen, A. *J. Phys. Chem. A* **1997**, *101*, 3589.

(21) Holmen, A.; Broo, A.; Albinsson, B.; Norden, B. *J. Am. Chem. Soc.* **1997**, *119*, 12240.

(22) Clark, L. B. *J. Phys. Chem.* **1995**, *99*, 4466.

(23) Rajendra, J.; Rodger, A. *Chem. Eur. J.* **2005**, *11*, 4841.

(24) Hughes, M. E.; Brandin, E.; Golovchenko, J. A. *Nano Lett.* **2007**, *7*, 1191.

(25) Chou, P. J.; Johnson, W. C. *J. Am. Chem. Soc.* **1993**, *115*, 1205.